# Fickian and Non-Fickian Diffusion with Bimolecular Reactions

**Brian Berkowitz, Yotam Berkowitz, Yaniv Edery, Harvey Scher**

**Department of Earth and Planetary Sciences**

WEIZMANN INSTITUTE OF SCIENCE

**Rehovot, Israel**

# Reaction-Diffusion Phenomena

- Relevance: geochemical systems (precipitation/dissolution, $CO_2$), physics, biology (cells)

- Bimolecular reactions: $A + B \rightarrow C$

- Treatment via partial differential equation (PDE) and particle tracking (PT) approaches
  (incorporation of effects of small-scale fluctuations!!!)

- Diffusion mechanism: Fickian, non-Fickian ("anomalous")

- Reaction term:
  PDE, Fickian: $\Gamma c_A c_B$, with $\Gamma$ a reaction constant
  PDE, non-Fickian: analytically intractable

- Particle Tracking: Continuous Time Random Walk (CTRW)
  $\rightarrow$ effectively quantifies anomalous transport and diffusion

# Reactions: Averaging Effects

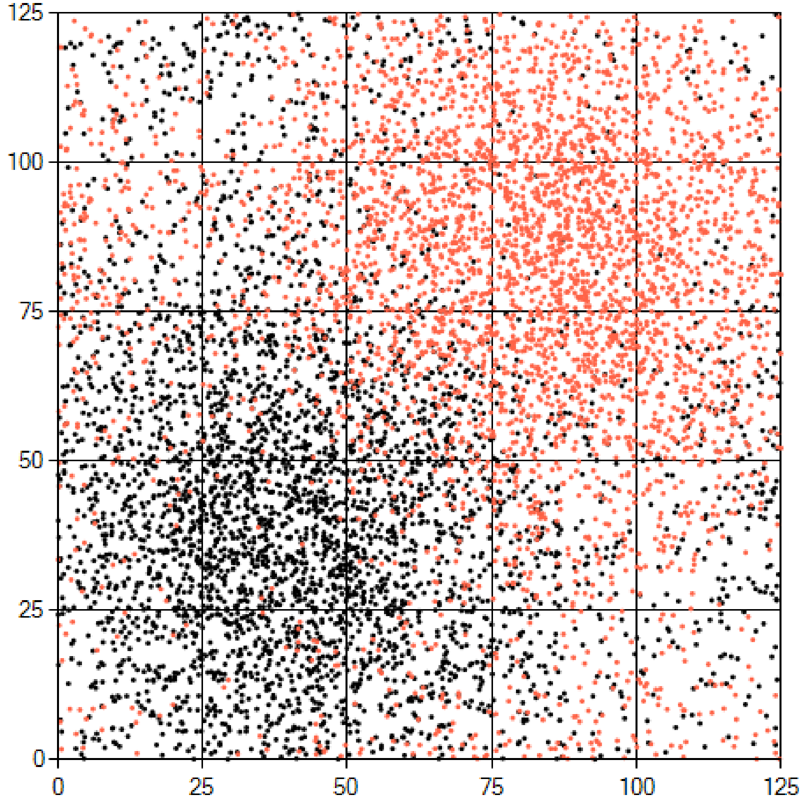


smaller $R$

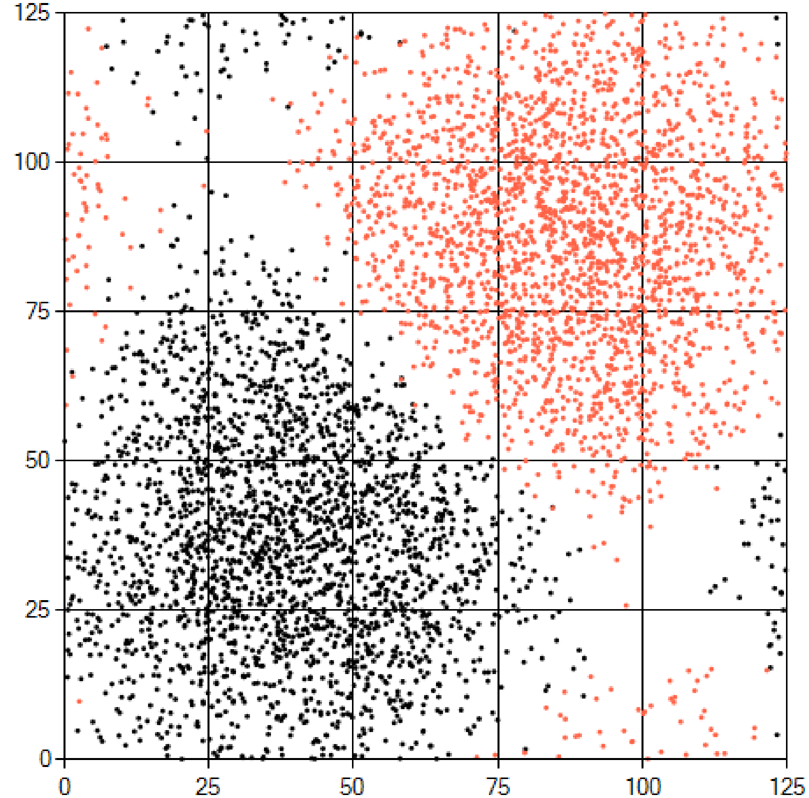


larger $R$

*A* and *B* diffuse, initially injected at separated points. Production of *C* (not shown) occurs when *A*, *B* are within a reaction radius *R*, which sets the small scale.

Small *R* enhances interpenetration of *A*, *B*.
Large *R* (= faster reaction rate) leads to a sharp reaction front
→ limiting mixing, but due to greater reaction

# <u>Question:</u> For point injection of reactive species *A* and *B*, what are patterning dynamics of product $A + B \rightarrow C$?

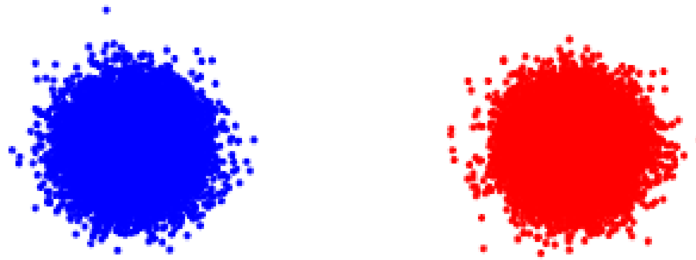

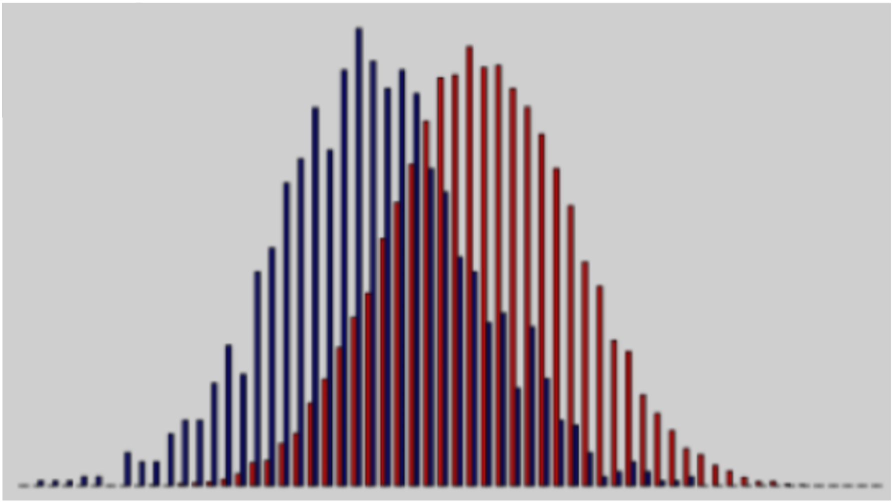

- Concentration profiles for Fickian / non-Fickian diffusion?
- *C* may precipitate (immobile) or remain in solution (diffuse)

# Modeling: CTRW Particle Tracking

- Particle tracking advantage: can study influence of small-scale fluctuations in species concentrations on reaction mixing and pattern formation (localized, pore-scale nature of reactions)

- Continuous Time Random Walk (CTRW): easily accounts for Fickian and non-Fickian diffusion

- $$\mathbf{s}^{(N+1)} = \mathbf{s}^{(N)} + \varsigma^{(N)}, \quad t^{(N+1)} = t^{(N)} + \tau^{(N)}$$

$\mathbf{s}^{(N)}$, $t^{(N)}$ denote location of a particle in space-time after $N$ steps; spatial $\varsigma^{(N)}$ and temporal $\tau^{(N)}$ random increments assigned to particle transitions via a joint probability density $\psi(\mathbf{s}, t)$

Decoupled form: $\psi(\mathbf{s}, t) = \mathrm{p}(\mathbf{s})\,\psi(t)$ [independent pdf's]

***Temporal pdf controls the character of the diffusion***

# Modeling Aspects

Spatial: normal distribution for $p(s)$, radially uniform angular component

Temporal:

Fickian diffusion: $$\psi(t) = \lambda_t \exp(-\lambda_t t)$$ [mean = $1/\lambda_t$]

Non-Fickian diffusion, Truncated power law: $$\psi(t) = \frac{n}{t_1} \exp(-t/t_2)/(1 + t/t_1)^{1+\beta}$$

$0 < \beta < 2$, measure of the degree of anomaly; $n$ normalization constant;

$\psi(t) \sim (t/t_1)^{-1-\beta}$ for $t_1 \ll t \ll t_2$; $\psi(t)$ decreases exponentially for $t \gg t_2$

- Diffusion: $D = \varepsilon^2 / (4\delta t)$; with $\varepsilon$, $\delta t$ = mean step length, transition time
- Choose $D = 10^{-9}$ m$^2$/s (Fickian: normal $p(s)$, mean $\varepsilon = 10$ μm, $\sigma = 1$)
- 50,000 particles each of $A$, $B$; injection points separated by 100 μm
- Non-Fickian: $\beta = 0.7$, $t_1 = \delta t$ (median transition step matched to Fickian), $t_2$ large
- Reaction radius: $R = 0.1$ μm
- $C$ particles immobile (in cases shown here)

# Concentration Patterns and Profiles

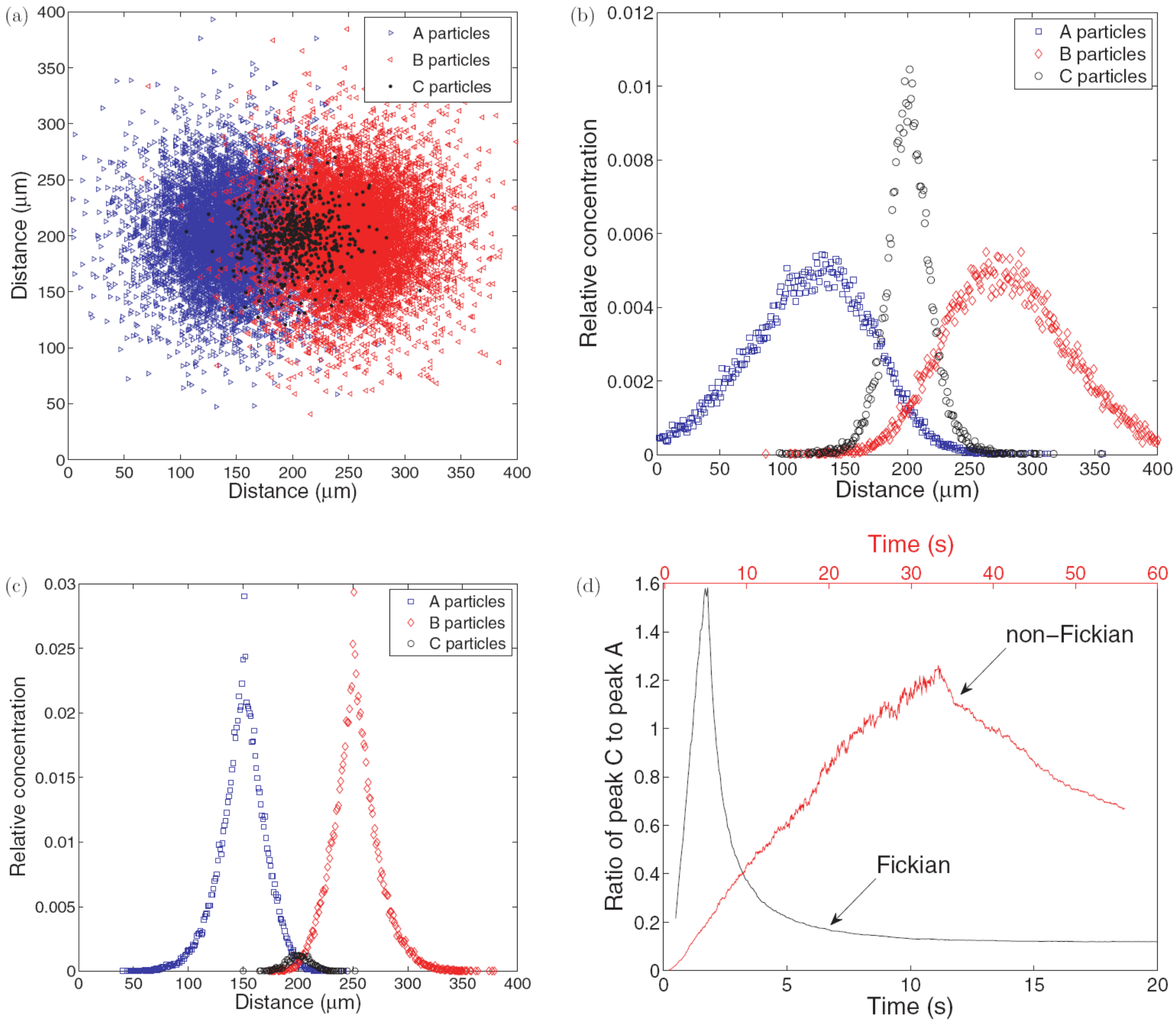


(a) Representative spatial *A* and *B* plume patterns, interacting to produce *C* (T = 15 s) for Fickian diffusion.

(b),(c) Spatially integrated (over *y* axis) concentration profiles of *A*, *B*, and *C* particles, at T = 2 s, for (b) Fickian diffusion and (c) non-Fickian diffusion with $\beta$ = 0.7.

(d) Ratios of peaks of spatially integrated *C* profile to *A* profiles, over time, for Fickian diffusion and non-Fickian diffusion.

# Rate of *C* Particle Production

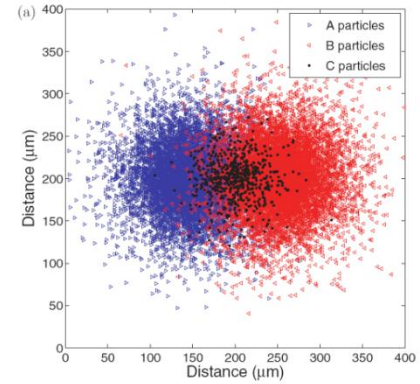


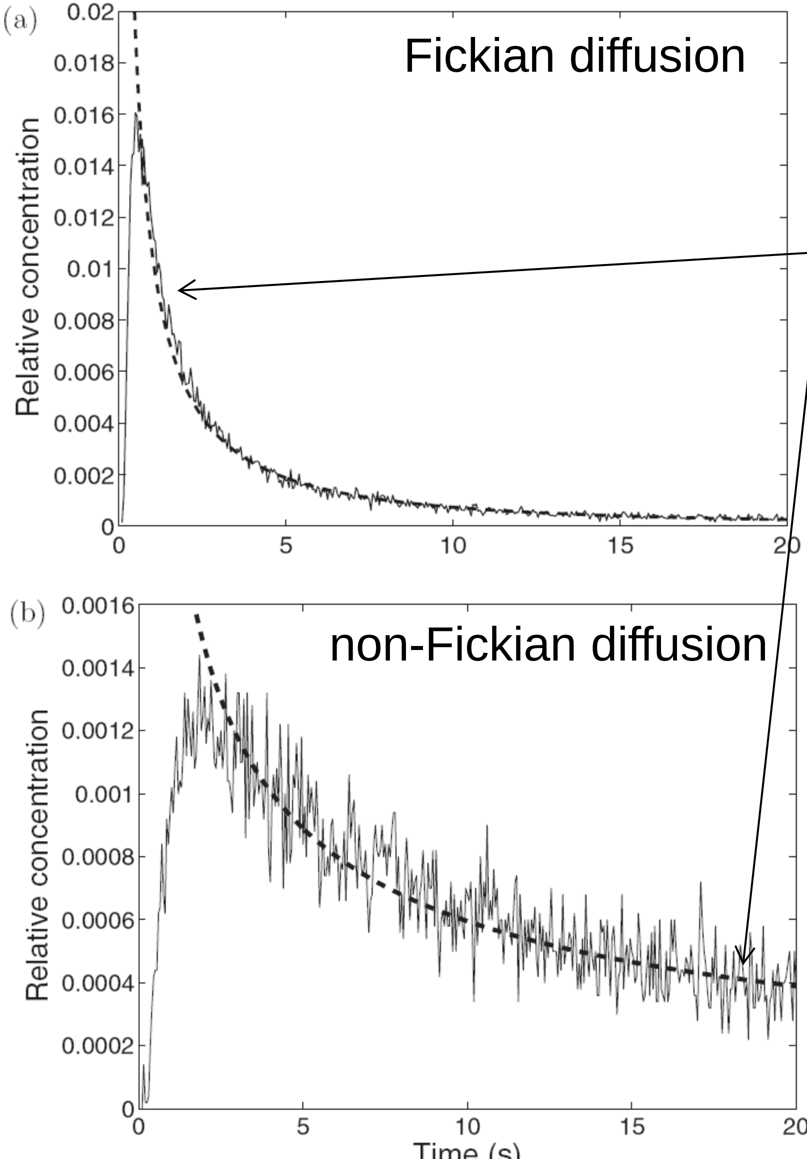


Dashed lines show fits of a <u>stretched exponential function</u>, $f(t) = \exp(-at^{\gamma})$
Fickian: $a = 4.54$, $\gamma = 0.20$
Non-Fickian): $a = 6.17$, $\gamma = 0.08$
[Note: *y*-axis scale larger for Fickian case]

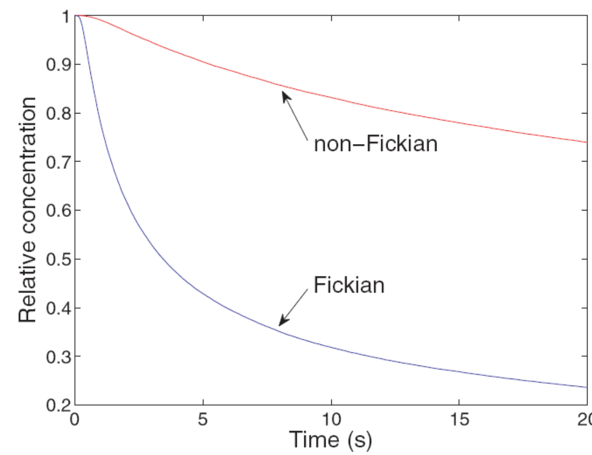


Corresponding decrease in relative concentration of *A* (or *B*) particles over time, for Fickian and non-Fickian diffusion.

# Gaussian and Lorentzian Characterization

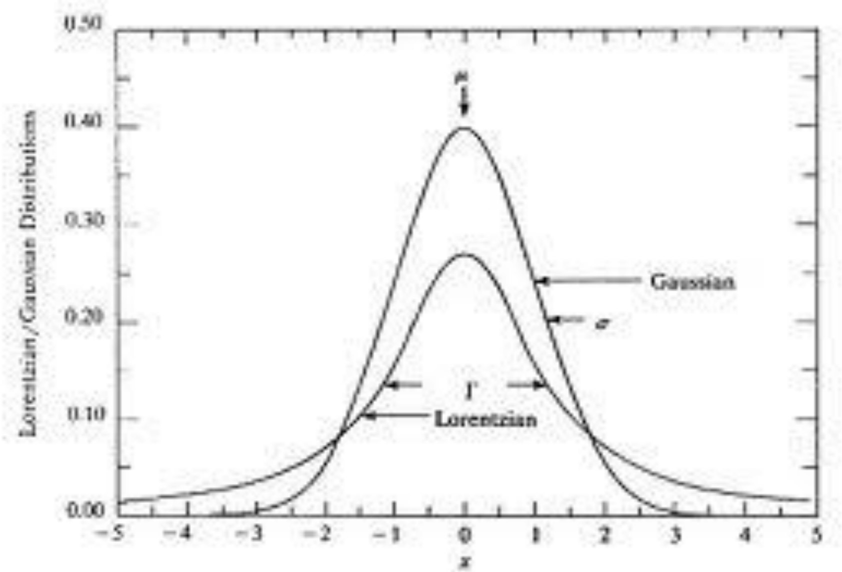


Gaussian distribution: compact

Lorentzian (Cauchy) distribution: heavy tailed (“broadening”)

*From previous figures, we expect C profiles to follow a two-time regime evolution.*

Consider a weighted sum of a Gaussian and a Lorentzian:

$$a \exp[-|x - 200|^2/(4dt^\alpha)] + b/[1 + c|x - 200|^2/(dt^\alpha)]$$

where $a$, $b$, $c$, $d$, and $\alpha$ are fitting constants.

**The relative weighting $a/b$ is the key parameter of interest.**

# *C* Particle Concentration: Spatial Profiles

Spatially integrated (over *y* axis) concentration profiles of (immobile) *C* particles:

Fickian:
(a) T = 2 s
(b) T = 15 s

non-Fickian:
(c) T = 2 s
(d) T = 15 s

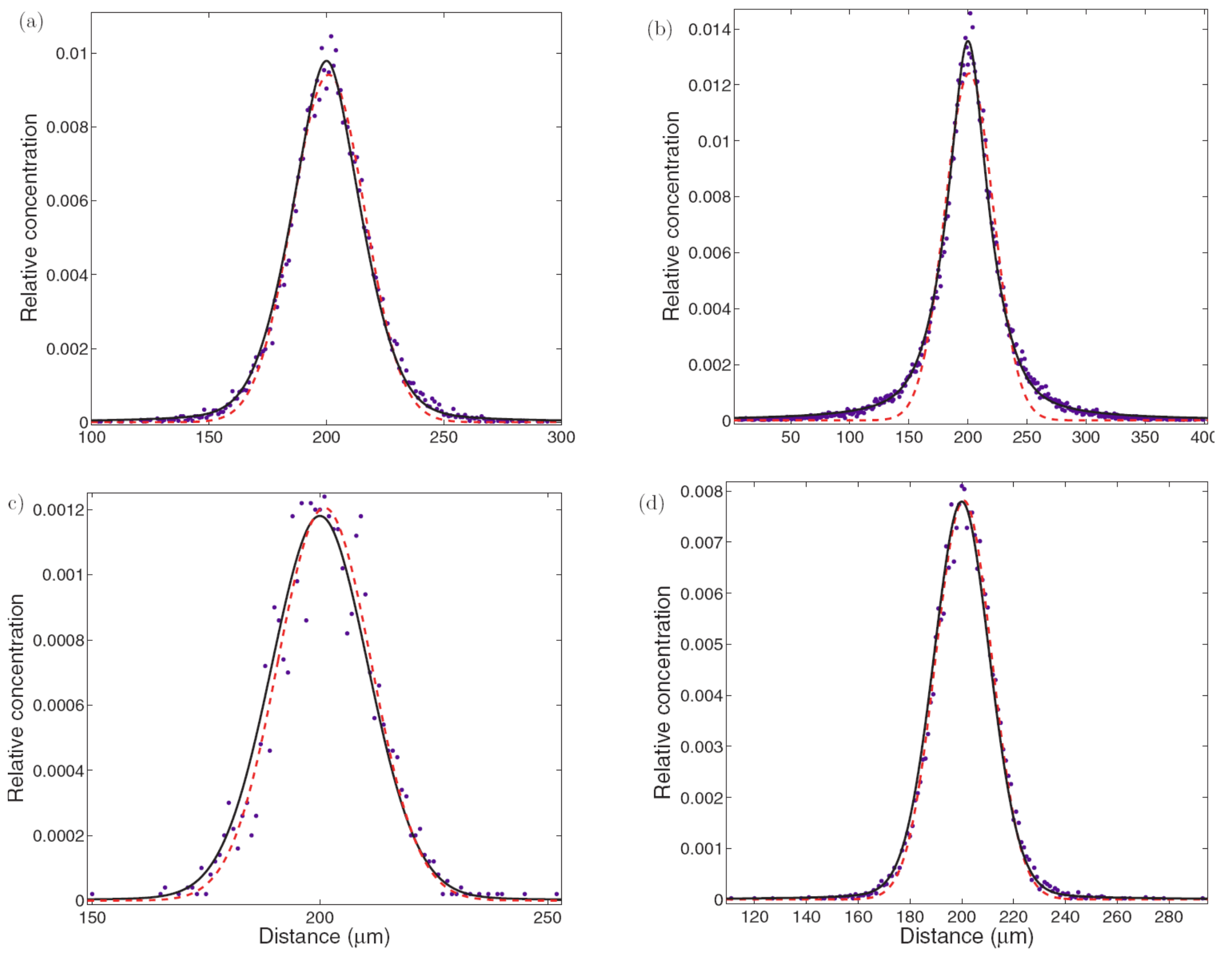


Profiles/curves are normalized by total number of *C* produced at the given time. Continuous curves show best fits of the weighted sum of **Gaussian** (weight $a$) and **Lorentzian** (weight $b$) distributions. Dashed lines (in red) are pure Gaussian fits.

**Ratios of weights $a/b$ (Gaussian/Lorentzian): (a) 2.1, (b) 0.3, (c) 12.8, and (d) 6.0.**

# Gaussian and Lorentzian Characterization

Fickian:

- Short times (a): profile reflects rapid compact growth in the reaction front region (= Gaussian)
- Longer times (b): *C* production builds up outside the reaction front region and the spatial extent of the profile spreads, with heavier tails
- $\Rightarrow$ *C* profile for Fickian diffusion evolves, transiting from a compact Gaussian to a heavy tailed Lorentzian

non-Fickian:

- Over same time range, *C* profile remains Gaussian; $a/b$ also decreases in time, but on a much larger time scale
- Difference in reaction patterns: a distinguishing feature of anomalous behavior (we do not detect $a/b$ < 1 out to T = 55 s)

Experiment interpretation:

- Appearance of a Gaussian *C* profile does not prove that the diffusion process is Fickian!
- Can detect non-Fickian diffusion by comparing *C* profile dynamics to calculated expectations based on normal diffusion.

# Additional Findings

- For <u>mobile</u> *C* particles (diffusing with same rules as *A* and *B*):
  *<u>Fickian case</u>:* suppresses fluctuations and Gaussian behavior persists
  *<u>non-Fickian case</u>:* *C* profiles have equal weights of Gaussian and Lorentzian components
- Times, distances show representative behaviors; larger and smaller (200 and 50 μm) distances between *A* and *B* injection points yield similar behaviors, with appropriate scaling
- Initial *A* and *B* vertical strip distribution yield the same *C* particle distribution behavior; the point or strip injection is not relevant
  $\Rightarrow$ dynamics are basic phenomena which account for growth of concentration fluctuations, as the species numbers decline in the reaction front

# Conclusions

- Mixing zone dynamics of a reaction product *C* during diffusion of two species (*A* and *B*) are examined, using a 2D particle tracking model for the reaction $A + B \rightarrow C$, allowing for both Fickian and non-Fickian transitions.

- Basic *C* pattern dynamics – temporal evolution of the spatial profile and the temporal *C* production – are similar for both modes of diffusion. But the distinctive time scale for the non-Fickian case is very much larger.

- For immobile *C*, the spatial profile pattern is a broadening (Gaussian) reaction front evolving to a concentration-fluctuation dominated (Lorentzian) shape. The temporal *C* production is fit by a stretched exponential.

- Analyzing experiments: appearance of Gaussian *C* profiles does not prove that the diffusion process is Fickian.

Berkowitz et al., Phys. Rev. E 2013

# Origins of Anomalous Transport in Disordered Media: Structural and Dynamic Controls

**Yaniv Edery, Harvey Scher, Alberto Guadagnini and Brian Berkowitz**

**Department of Earth and Planetary Sciences**

WEIZMANN INSTITUTE OF SCIENCE

# Background

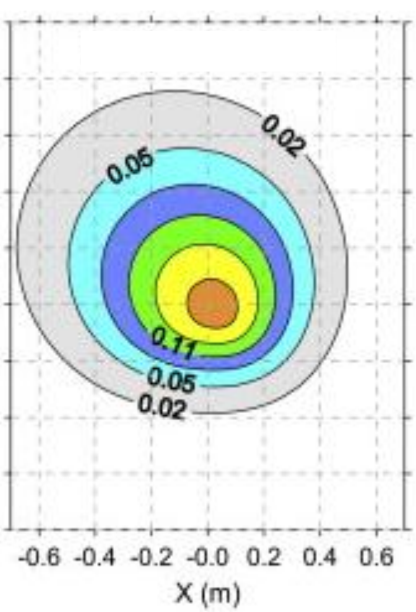


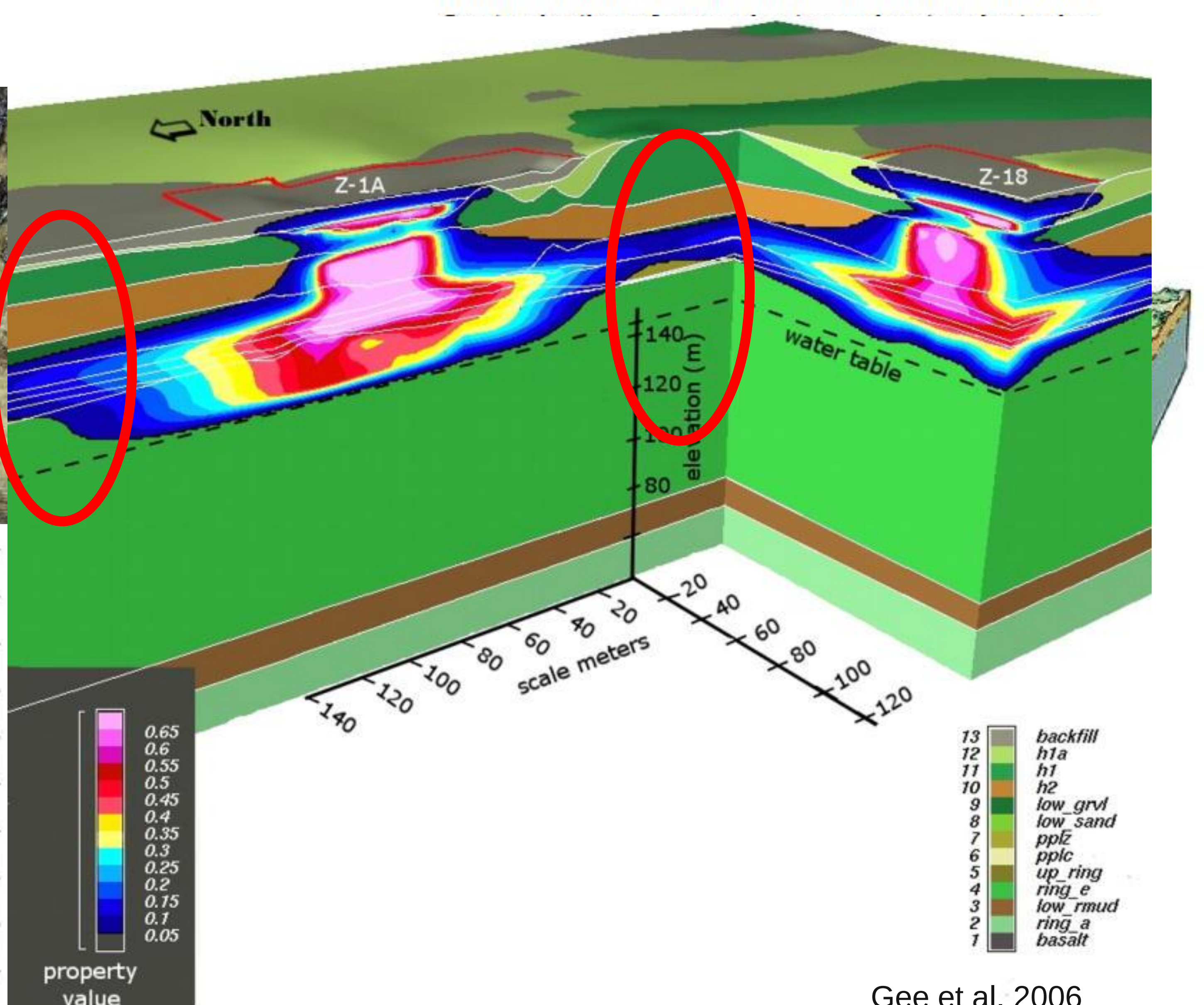


Gee et al. 2006

# Meter scale uniform sand: non-Fickian behavior

Even "homogeneous" systems are "anomalous"…

**Flow direction**

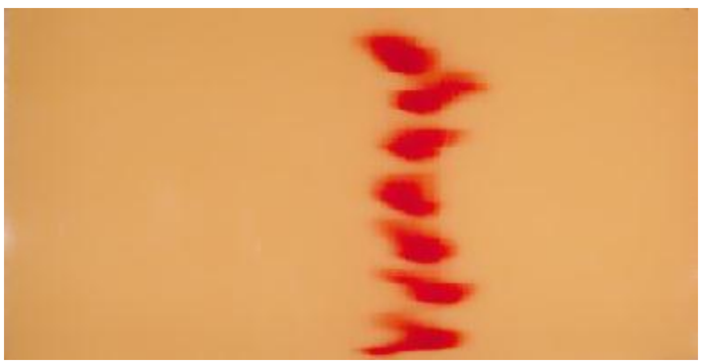

“Expected” Fickian:

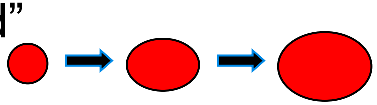

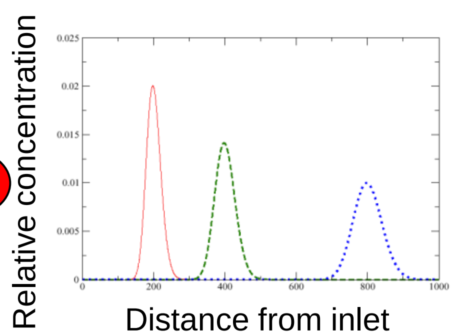


“Actual” non-Fickian:

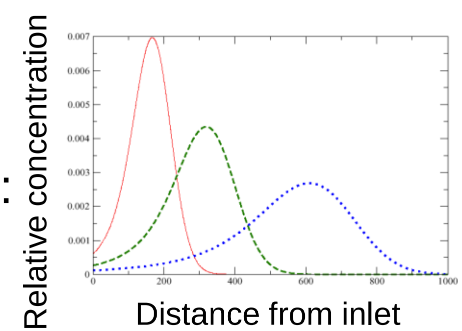

# Probabilistic Approach: Continuous Time Random Walk

- Transport: sequence of particle transitions (in space and time)
- $\psi(\mathbf{s},t)$: Probability density function (pdf)
- Account for rare events: non-Fickian transport

Generalized CTRW transport equation:

$$\tilde{M}(u) \equiv \bar{t}u\frac{\tilde{\psi}(u)}{1-\tilde{\psi}(u)}; \qquad u\tilde{c}(s,u) - C_0(s) = \tilde{M}(u)\left[v_\psi \cdot \nabla \tilde{c}(s,u) - D_\psi : \nabla\nabla \tilde{c}(s,u)\right]$$

Continuum approach: CTRW- PDE

Particle tracking: CTRW- PT

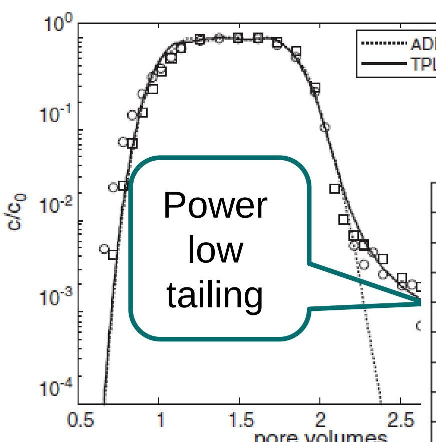


Rubin et al. 2012

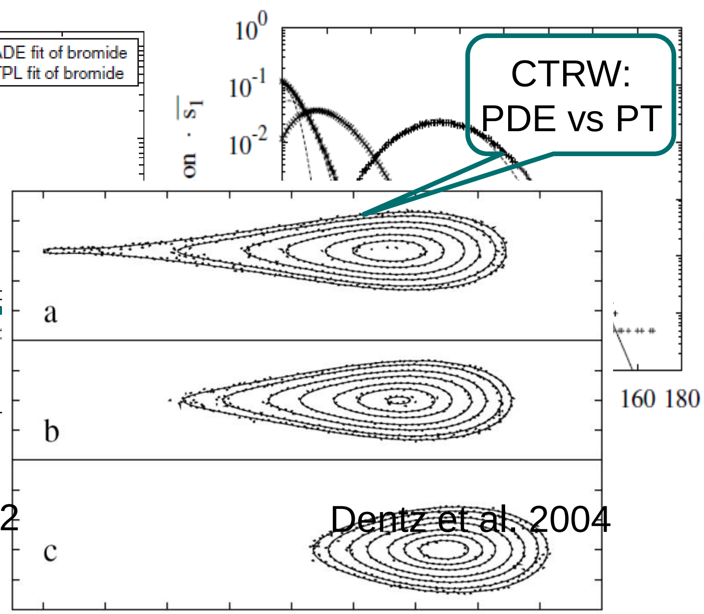


Dentz et al. 2004

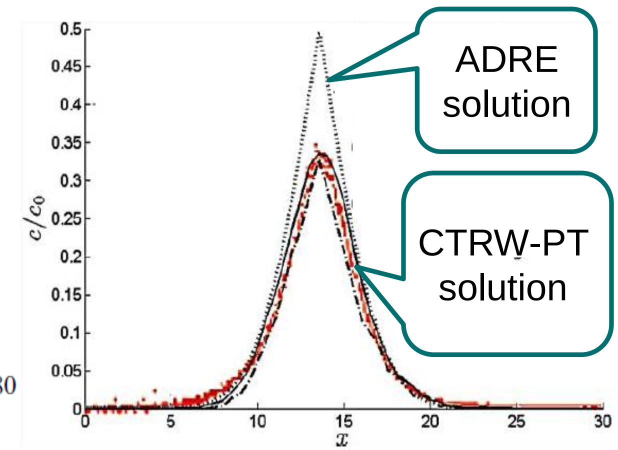


Edery et al. 2009

# Transit time distribution $\psi(t)$: truncated power law (non-Fickian to Fickian evolution)

$$\psi(t) = \frac{n}{t_1} \frac{\exp(-\tau/\tau_2)}{(1+\tau)^{1+\beta}}$$

$\tau \equiv t/t_1,\ \tau_2 \equiv t_2/t_1,\ 0 < \beta < 2$

$n$ = normalization constant

$\psi(t) \sim \tau^{-1-\beta}$ for $1 \ll \tau \ll \tau_2$

$\psi(t)$ decreases exponentially for $\tau \gg \tau_2$

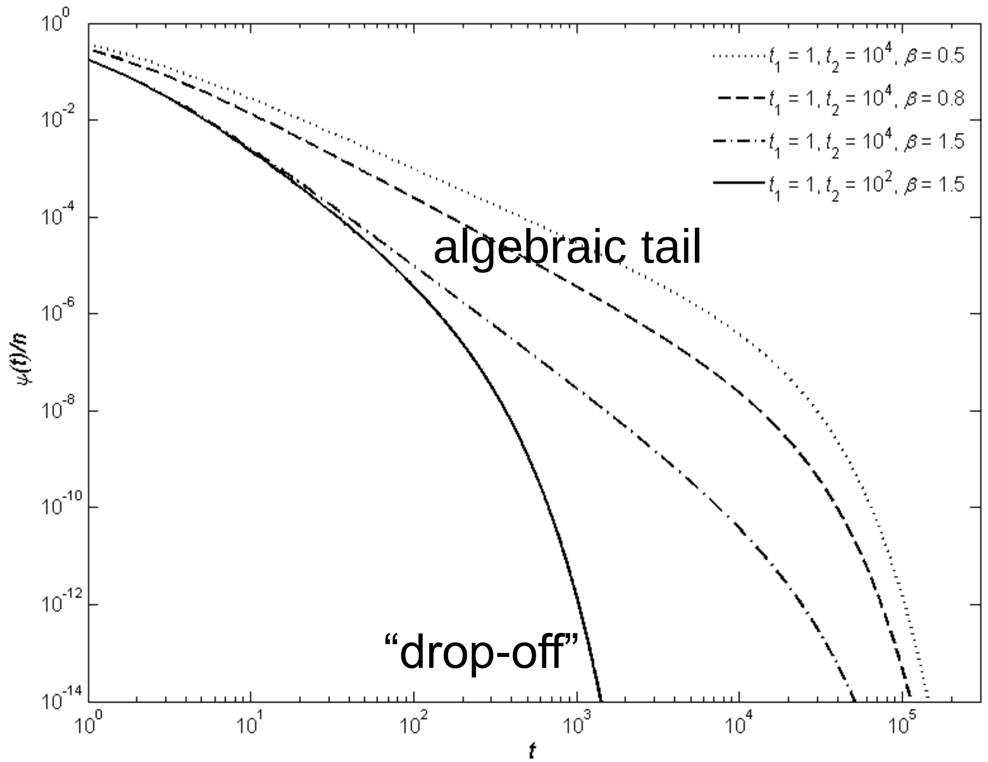


Note: (1) effect of cutoff time $t_2$, (2) algebraic tail, (3) drop-off (transition to Fickian)

*Evidence for power law pdf: theoretical analyses, semi-analytical analyses of permeability/flow fields, numerical simulations of fluid flow / tracer transport, fits to measured tracer breakthrough curves*

# Non-Fickian transport in heterogeneous porous media

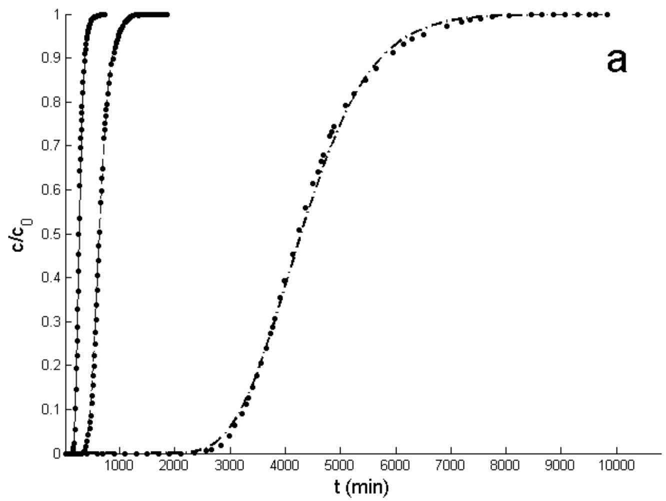


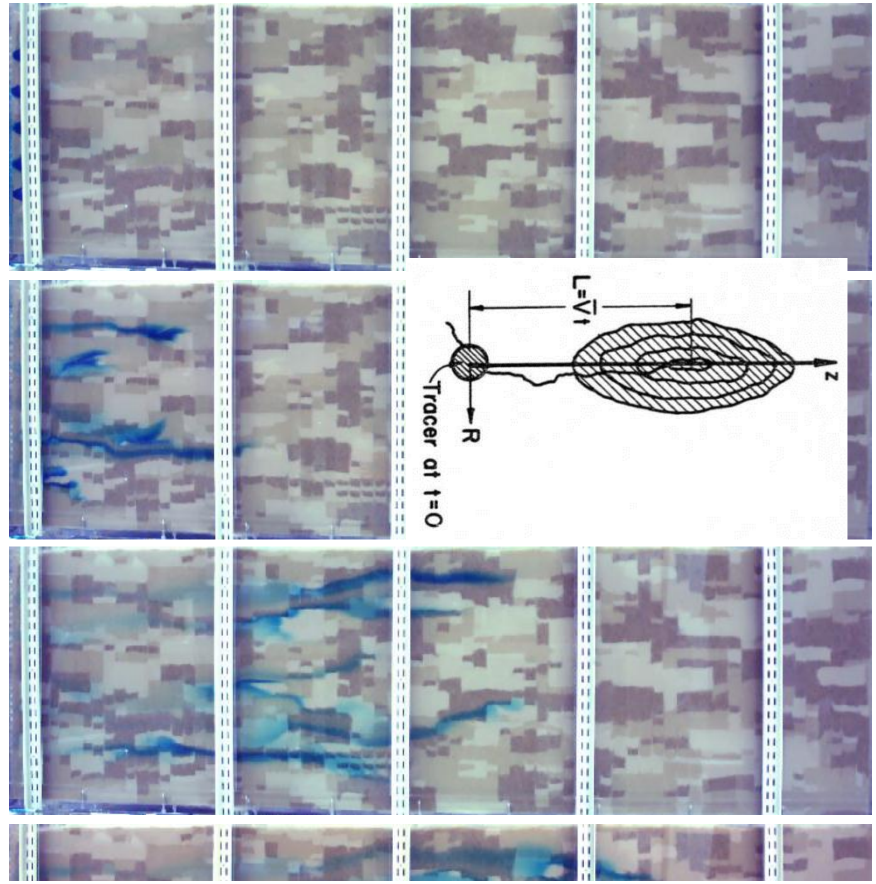


$$u\tilde{c}(\mathbf{s},u)-c_{\mathrm{o}}(\mathbf{s})=-\tilde{M}(u)\left[\mathbf{v}_{\psi}\cdot\nabla\tilde{c}(\mathbf{s},u)-\mathbf{D}_{\psi}:\nabla\nabla\tilde{c}(\mathbf{s},u)\right]$$

$$\psi(t)=\frac{n}{t_1}\frac{\exp(-t/t_2)}{(1+t/t_1)^{1+\beta}}$$

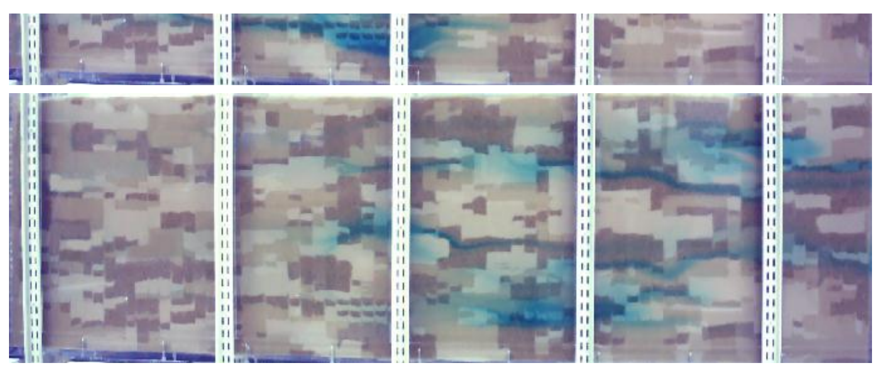

Levy and Berkowitz, J Contam Hydrol 2003

# Plume Evolution: $\psi(t)$ sampled at different residence times

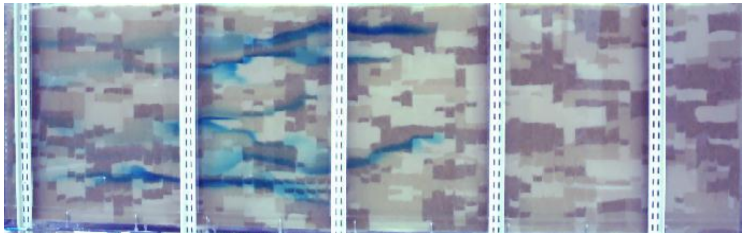

***Three experiments: flow rates 11, 74, 175 mL/min***

**Truncated power law $\psi(t)$:**
***constant exponent, parameter ratios for all curves***

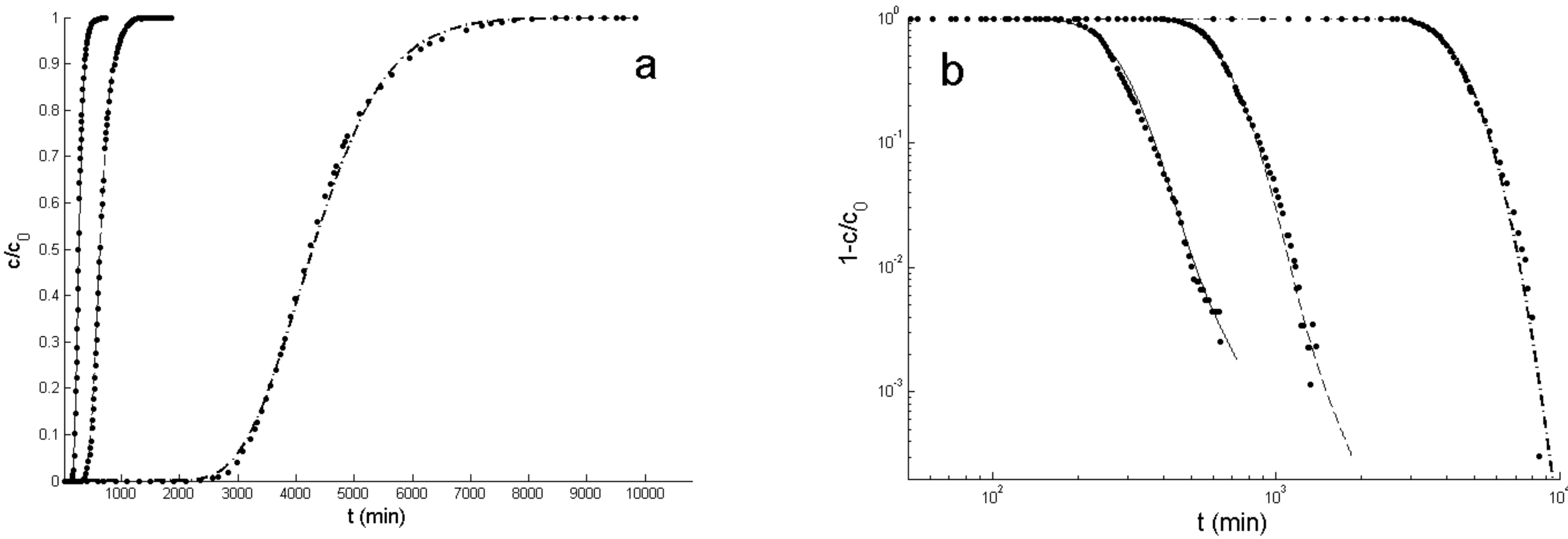


[ constant $\beta$, $v_\psi/D_\psi$, $v/v_\psi$, $t_1$, $t_2$; with $t_1 = s/v_\psi$ and $s \approx$ 15% average grain size ]

Berkowitz and Scher, AWR 2009

# Natural Heterogeneity: Transport Patterns "Revisited"

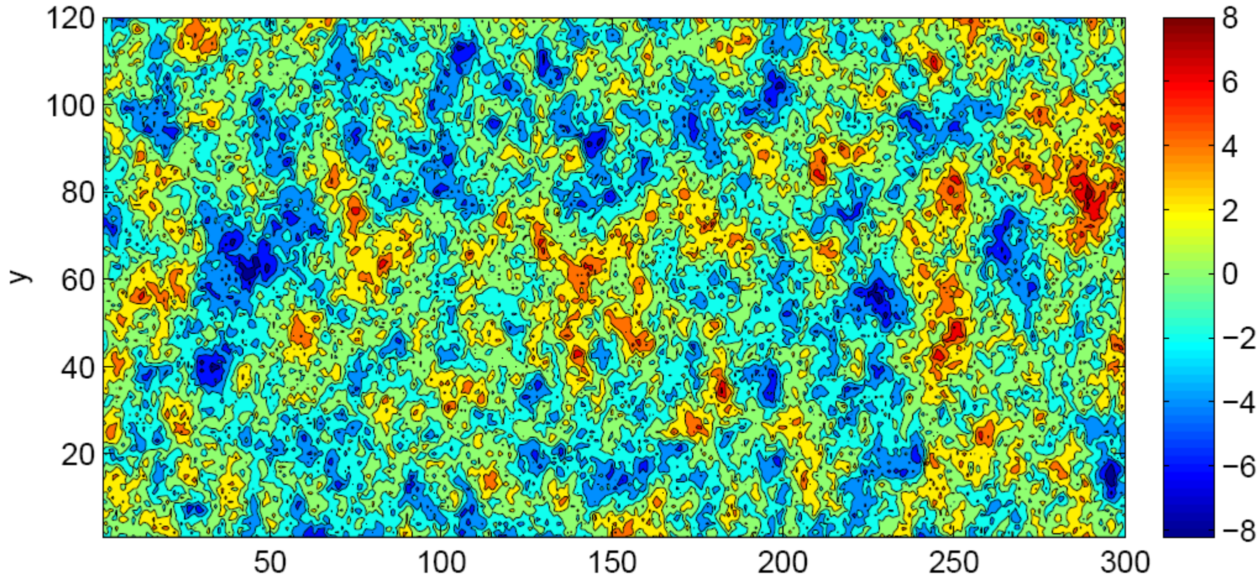


Spatial map of full *K* field; ln(*K*) variance $\sigma^2$=5

Statistically homogeneous and isotropic, multivariate Gaussian field

Color bar in ln(*K*) scale

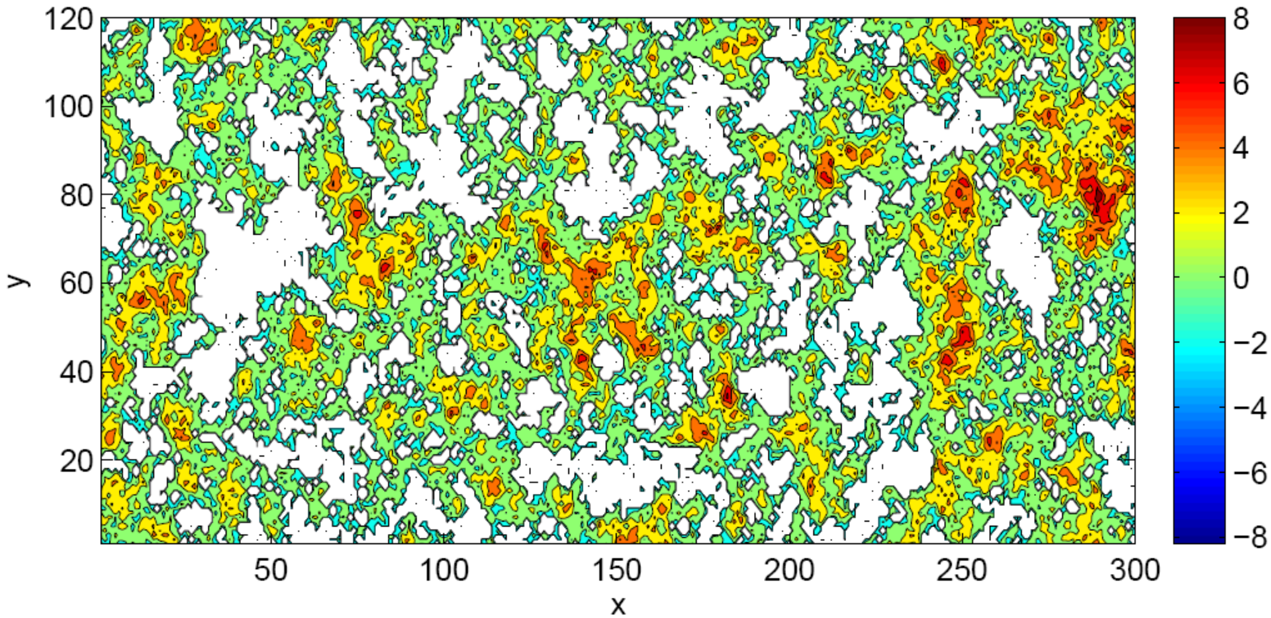


As above; critical path analysis (CPA); ln(*K*) < -0.63

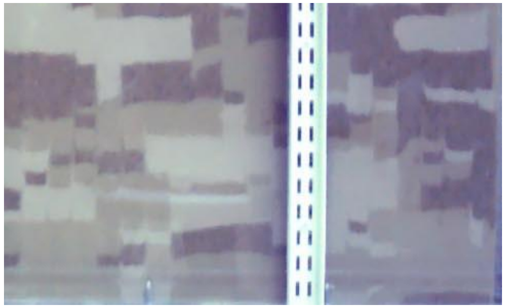

# Transport Patterns "Revisited": CTRW and ADE

(a)

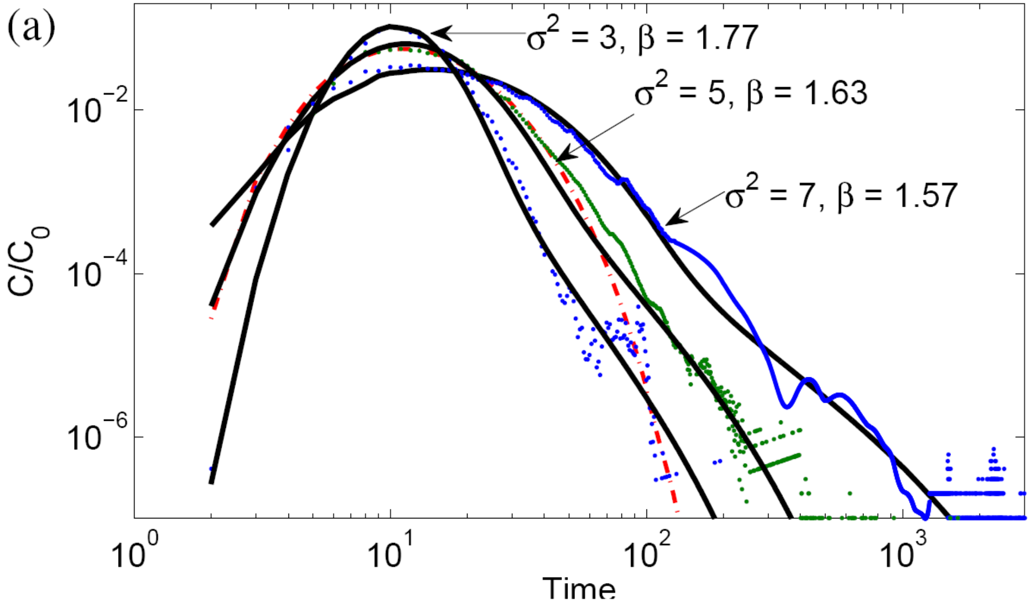


(b)

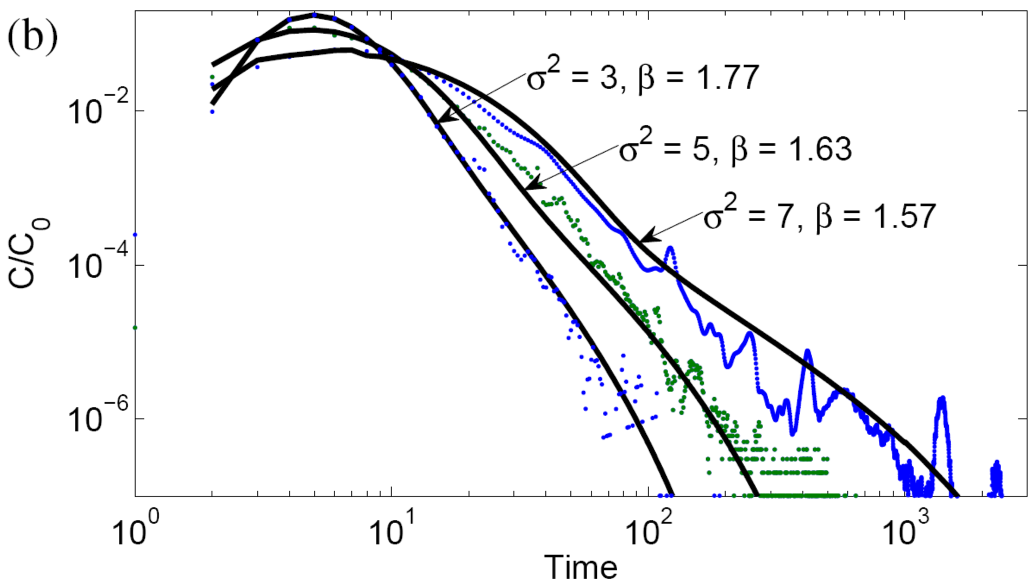


Ensemble (100 realizations) breakthrough curves (points) for three ln(*K*) variances and corresponding CTRW fits.

(a) Domain boundary (x=300)
(b) Domain midpoint (x=150)

Also shown: ADE for $\sigma^2$=5 (*v*=3.4; but average fluid velocity = 5.6)

Oscillations in tails caused by formation of limited set of preferential channels, leading to variations in the distribution of small numbers of particles arriving at outlet.

# Transport Patterns – Particle Interrogation of Domain

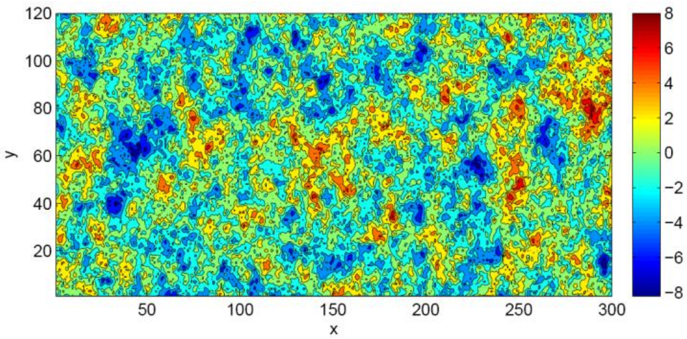


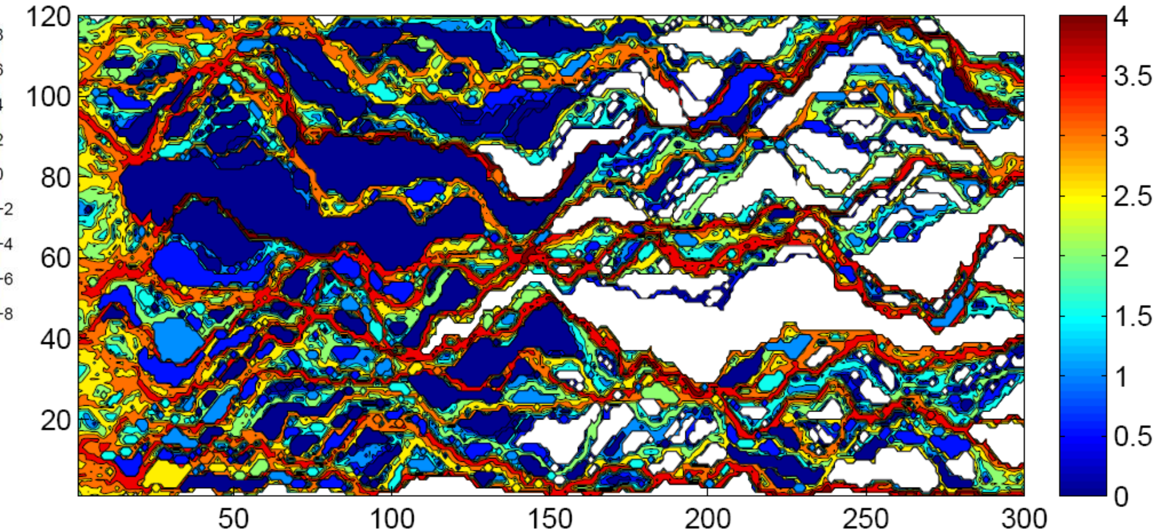

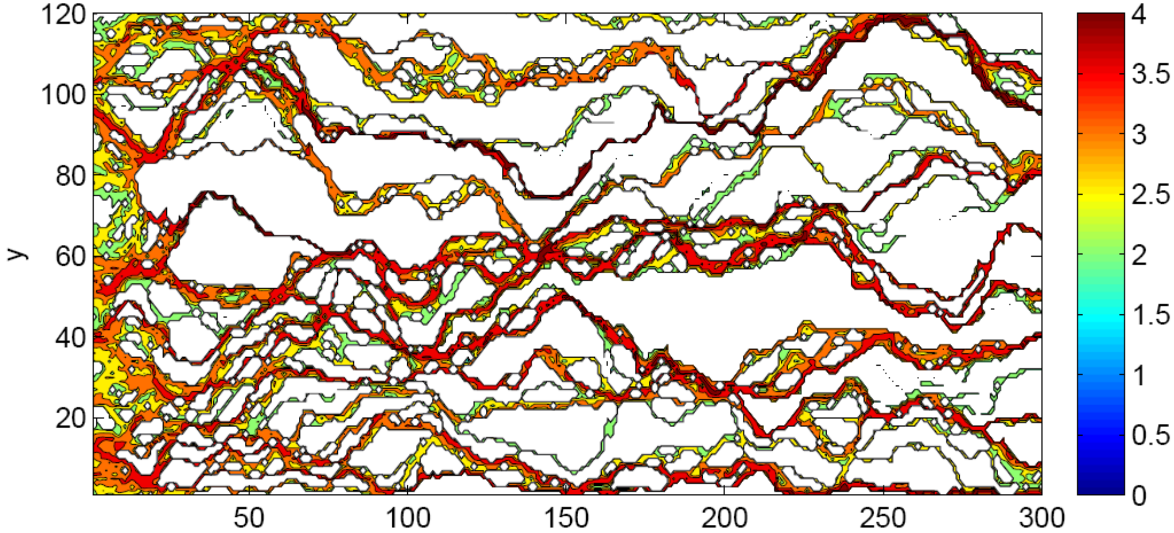


Upper: Particle paths (for $\sigma^2$=5). Note the formation of very limited set of preferential channels
Lower: Preferential particle paths (cells with visitation of >100 particles = 0.1% of all particles in domain)

# Natural Heterogeneity: Critical Path Analysis / Percolation

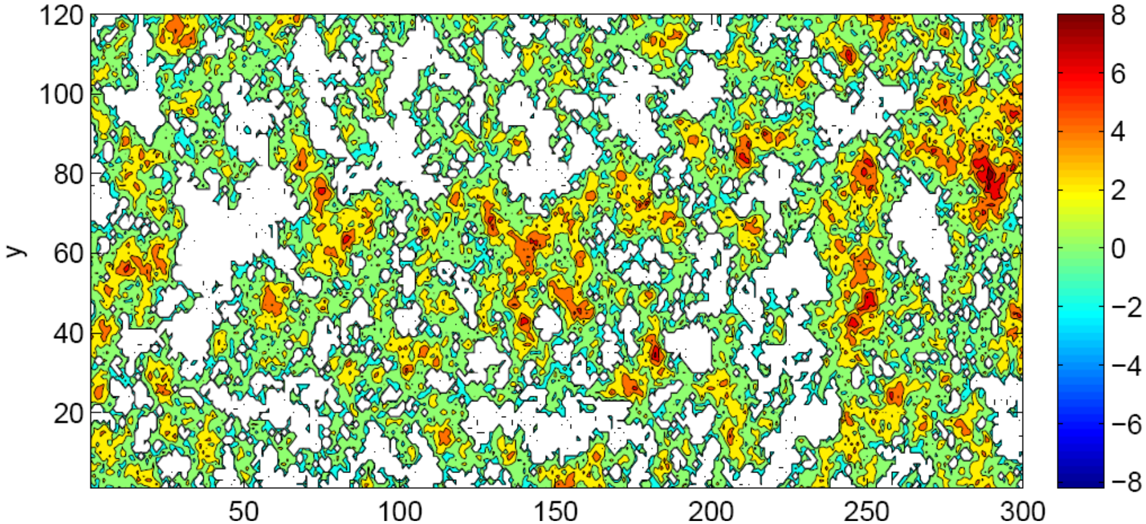


Color bar in ln($K$) scale

Note: *Inadequacy* of Critical Path Analysis (*based only on structure*)

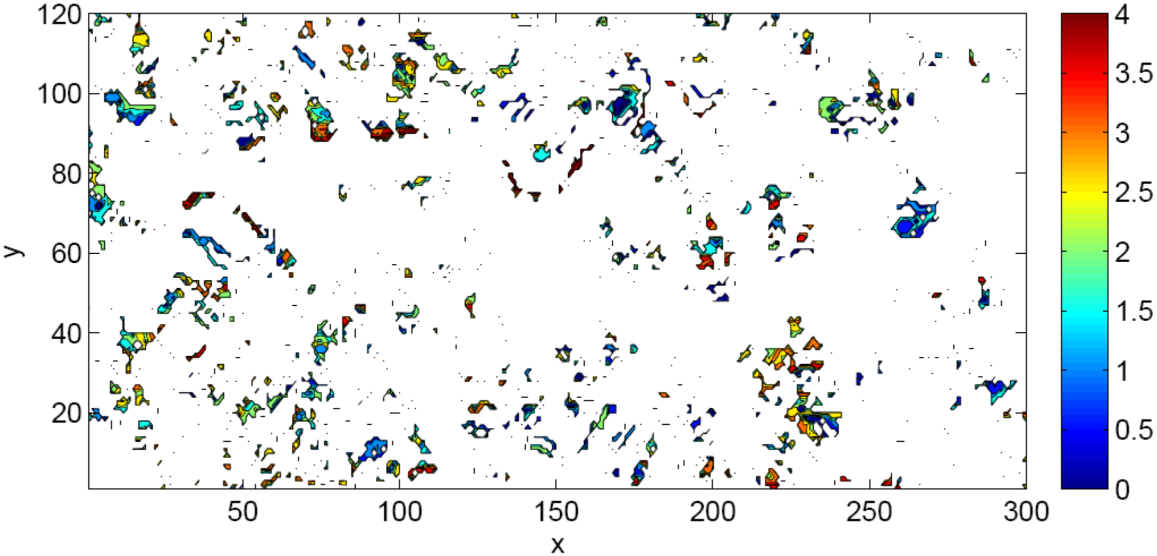


Cells with Low Conductivity Transitions (LCTs) of particles are a major, controlling factor!

Effect of $K$ (or $v$) correlations: embedded in preferential paths, but they do not "predict" the low conductivity transitions.

Upper: Spatial map of full $K$ field; ln($K$) variance $\sigma^2$=5. Critical path analysis (CPA); ln($K$) < -0.63
Lower: Low conductivity transition cells (below CPA)

# Natural Heterogeneity – Effective Conductivities

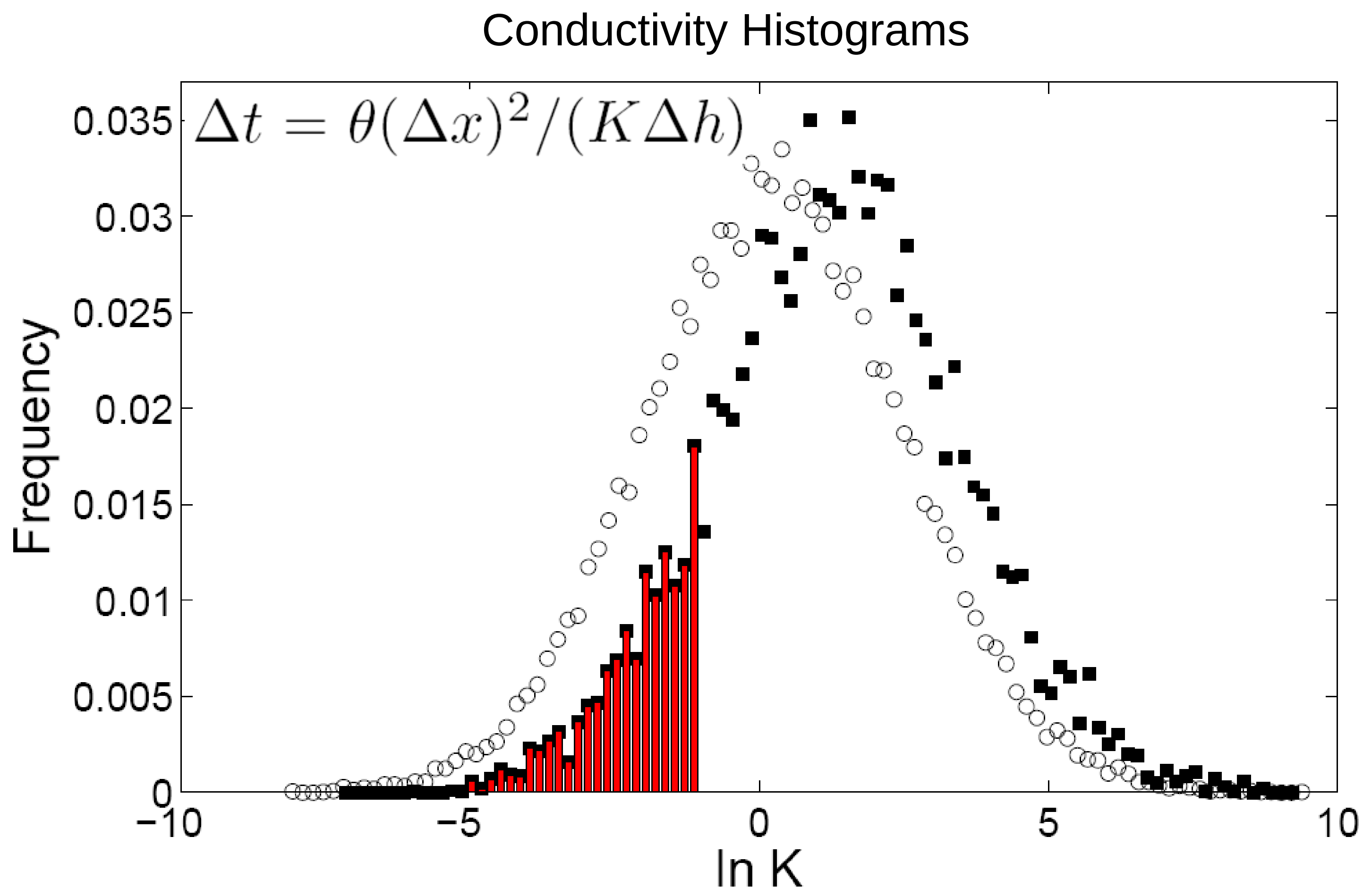


Open circles: normalized by the number of cells, for spatial map of full *K* field; $\sigma^2$=5; mean ln(*K*)=0.26, skewness 0.03

Filled squares: preferential particle paths, weighted and normalized by number of particles visiting in each cell, {*wK*}; weighted mean ln(*K*)=1.43, skewness 3.89 Bars in red indicate frequency of LCTs.

# Natural Heterogeneity – CTRW Transport Description

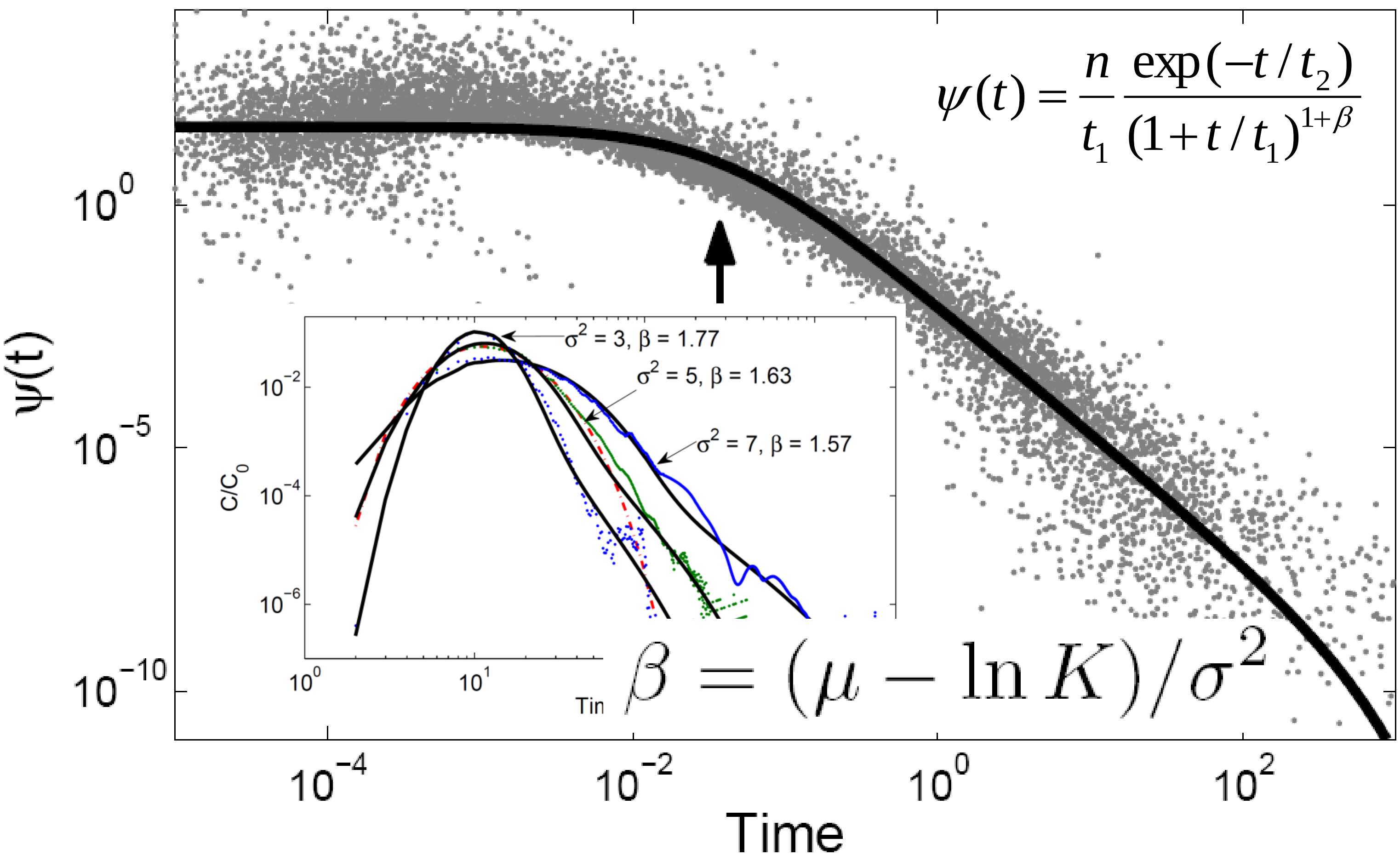


Ensemble particle-weighted conductivity histogram ($\sigma^2$=5, 100 realizations); based on conductivity histrogram, transforming to particle transition time distribution within cells, representing $\psi(t)$ vs. $t$.
Solid curve shows the TPL with same values for breakthrough curve shown in inset.
Arrow marks $t_1$, the onset of the power law region at $t_1 < t < t_2$, corresponding to ln($K$) < -1.

# Natural Heterogeneity – Connecting Conductivity and Transport

From conductivity histogram: determine an average head gradient over each cell (weighted by relative number of visiting particles). Then determine average residence times in these cells, for each *K* bin, with Darcy's law:

$$\Delta t = \theta(\Delta x)^2/(K\Delta h)$$

$\Rightarrow$ obtain a frequency (weighted by relative number of visiting particles) of particle residence times in all domain cells

***RESULT***: statistical analysis of particle paths, which renders, the weighted *K* distribution (previous slide), leads directly to the CTRW $\psi(t)$ !!

Functional form of weighted time distribution:

$$f = n_k \exp[-(\ln K - \mu)^2/(2\sigma^2)]/t$$

Equate log derivative to that of TPL to develop an analytical expression for $\beta$ in terms of the weighted *K* histogram parameters:

$$\beta = (\mu - \ln K)/\sigma^2$$

# Conclusions

- “Origin” of anomalous transport: we develop a direct connection between CTRW parameters and the randomly heterogeneous hydraulic conductivity field.
- Transport cannot be explained solely by the structural knowledge of the disordered medium; dynamic/flow controls are critical factors. Low conductivity transition zones largely determine the preferential flow paths.
- A basic determinant of the distribution of local transition times, which defines the transition time pdf used in the CTRW description, is a conductivity histogram weighted by the particle flux. Agreement between simulations, pdf parameters, and matches to BTCs is convincing.
- A quantitative relationship between the power law exponent $\beta$ and the statistics of the underlying (correlated) hydraulic conductivity field has been determined.
- Models based on critical path analysis and percolation theory are not applicable: the power law region of the transition times that controls the anomalous transport behavior lies below the critical path threshold.
- Use of advection-dispersion equation: particle plume convergence to this model is not due to “homogenization” of the plume sampling in the domain, but rather to focusing of flow in a limited number of relatively uniform preferential pathways.

Edery, Guadagnini, Scher, Berkowitz (WRR, 2014)